SMAR 2015 – Third Conference on Smart Monitoring,
Assessment and Rehabilitation of Civil Structures

Design criterion for fatigue strengthening of steel girders using bonded CFRP laminates

Elyas Ghafoori[1,4], Masoud Motavalli[1], Alain Nussbaumer[2], Xiao-Ling Zhao[3], Mario Fontana[4]

[1] Empa, Swiss Federal Laboratories for Materials Science and Technology, Structural Engineering Research Laboratory, Dübendorf, Switzerland.
[2] EPFL, Swiss Federal Institute of Technology Lausanne, Steel Structure Laboratory (ICOM), Lausanne, Switzerland.
[3] Monash University, Department of Civil Engineering, Wellington Rd., Clayton, VIC 3800, Australia.
[4] ETH Zürich, Institute of Structural Engineering (IBK), Zürich, Switzerland.

ABSTRACT: Aging steel structures are one of the common problems that structural engineers are facing today. Several studies have shown that strengthening of steel members using carbon fiber-reinforced polymer (CFRP) laminates can increase the load carrying capacity and the design fatigue life of steel members. This paper presents the results of a study on the fatigue strengthening of steel beams with bonded CFRP laminates. The principle of constant life diagram (CLD) methodology is explained. An analytical solution is developed to predict the fatigue resistance of steel beams after strengthening with bonded CFRP laminates. The method is capable to determine the required geometrical and mechanical properties of the strengthening element such that the steel detail is shifted from a finite-life regime to the infinite-life regime. In order to validate the model, five steel beams, including one reference beam and four strengthened beams were tested under cyclic loadings. The beams were strengthened with normal modulus (NM), high modulus (HM) and ultra-high modulus (UHM) laminates. It was shown that the developed analytical model can be used to choose the most effective fatigue strengthening solution.

1 INTRODUCTION

Although there have been many studies on fatigue strengthening using CFRP materials (e.g., Colombi et al. (2003), Täljsten et al. (2009), Wu et al. (2013)), nearly all of these studies have used CFRP for strengthening ‘cracked’ steel members to reduce or arrest fatigue crack growth (FCG). In this type of studies, the assessed steel specimens typically had a pre-crack of a certain crack length, which simulated the presence of a real crack. The results of such studies have shown that CFRP could reduce the FCG rate by reducing the overall stress intensity factor (SIF) at the crack tip, which could lead to a longer fatigue life. In other studies, the overall SIF at the crack tip was reduced to below threshold SIF generated by the pre-stressed CFRP laminates. Note that the concept of the threshold SIF is normally used in damage-tolerant designs and defines the loading criterion under which the cracks grow negligibly.

The concept of the fatigue limit, which is the focus of this paper, is often used in the fatigue resistance design approach and determines the loading criterion under which no cracks form. Ghafoori et al. (2015b), Ghafoori et al. (2015a) and Ghafoori (2015) developed a method based on the fatigue resistance design approach, and determined the minimum CFRP pre-stress level required to prevent fatigue crack initiation. It was theoretically and experimentally demonstrated that by applying a compressive force to a metallic detail using a pre-stressed CFRP laminate, the stresses can be shifted below the fatigue limit so that no cracks will form. In this paper, a closed-form analytical solution was developed to predict the stresses in the beams strengthened by the pre-stressed CFRP laminates. Different mechanisms by which the stresses were shifted from the risky ‘finite-life’ region to the safe ‘infinite-life’ region are explained. The results of the analytical solution are compared with the results of a series of static and fatigue experiments.

2 THEORITICAL BACKGROUND

2.1 Fatigue criteria

Figure 1 shows a CLD that defines the three main stress regions. The middle region bounded by R=0 and R=±∞ is for tension-compression (T-C) stresses, the right region bounded by R=1 and R=0 is for tension-tension (T-T) stresses, and the left region bounded by R=±∞ and the horizontal axis is for compression-compression (C-C) stresses. The level of the fatigue failure probability has also been schematically illustrated by different markers. The green triangle marker shows the safe zone, in which no cracks will form. The yellow square marker indicates the risky zone, where cracks may form with approximately a 50% probability. The red circular marker shows the unsafe region, where cracks will form with a probability of more than 50%.

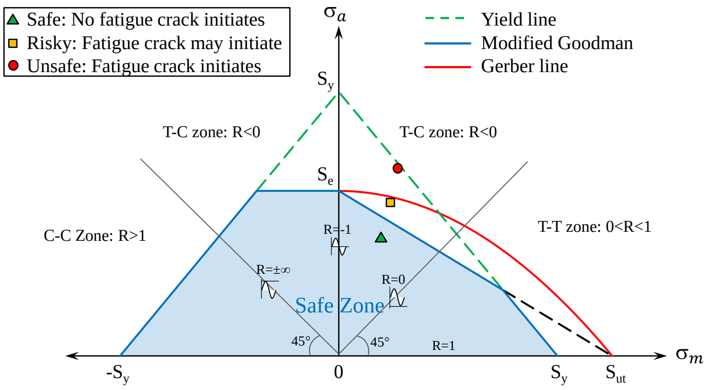

Fig. 1. Stress regions of tension–tension (T-T) with 0 < R < 1, tension–compression (T-C) with R < 0 and compression–compression (C-C) with R > 1 (Ghafoori 2015).

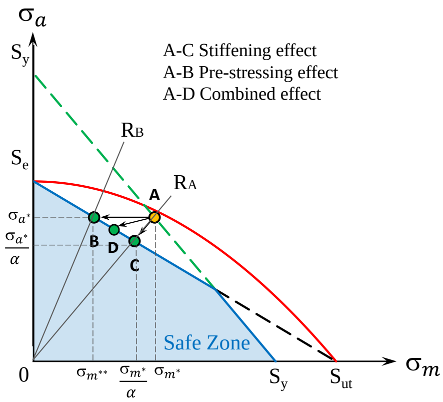

Fig. 2. Shifting the stresses from the risky to the safe region through the A-B path, the A-C path or the A-D path.

Based on extensive experimental analysis, Goodman proposed a straight line through σ_a =S_e and σ_m =S_{ut}, with criterion equation (Budynas and Nisbett 2008)

$$\frac{\sigma_a}{S_e} + \frac{\sigma_m}{S_{ut}} = \frac{1}{n} \tag{1}$$

where S_e is the fatigue endurance limit, n is the safety factor, S_{ut} is the ultimate strength, and σ_m and σ_a are the mean and alternating stresses. Ghafoori et al. (2015a) showed that the modified Goodman criterion is conservative enough to prevent fatigue failure in ductile metals strengthened with CFRP laminates and can be used for design purposes.

2.2 Increasing the fatigue life by reducing the mean stress

Assume that a beam is subjected to cyclic loading and that the mean and alternating stresses at the beam bottom flange before strengthening are σ_{m*} and σ_{a*}, as shown by point A in Fig. 2. The beam will be then strengthened by pre-stressed NM CFRP laminates, and the mean stress will be shifted to σ_{m**}, while the stress amplitude will decrease only negligibly. The NM laminates due to their relatively smaller Young's modulus (compared to that of steel) often cannot decrease the alternating stress substantially. Path A-B in this figure shows the effect of the pre-stressed NM CFRP, by which the mean stress level can be considerably decreased but the stress amplitude is decreased only negligibly. Due to the applied compressive stress, the stress ratio is reduced from R_A to R_B (i.e., $R_B<R_A$). Point B is in the safe zone, such that the metallic member will have an infinite fatigue life.

2.3 Increasing the fatigue life by increasing the stiffness

In this section, it is shown that it is also possible to increase the fatigue life of a metallic beam by increasing the stiffness of the metallic member using non-prestressed UHM CFRP laminates. By bonding the UHM CFRP laminates to the beam's bottom flange, the stiffness of the beam is increased. In this way, the minimum and the maximum stresses are reduced by a factor of α ($\alpha > 1$). Therefore, the stress amplitude and the mean stress will also be reduced by the same factor, σ_{a*}/α and σ_{m*}/α as shown in Fig. 2. In Fig. 2, path A-C shows the stiffening effect. Point C is in the safe zone, so this detail will have an infinite fatigue life under the applied cyclic loads. Note that stiffening can be accomplished in several ways, such as by increasing the thickness, the width or the Young's modulus of the CFRP laminate.

When the beam is strengthened by a pre-stressed UHM laminate, a combined effect of decreasing of both the mean and alternating stresses will be achieved. This is shown by point D in Fig. 2. The shortcoming of this method is that UHM laminates are often brittle and difficult to use in pre-stressing solutions.

3 DETERMINATION OF RETROFITTING PARAMETERS TO PREVENT FATIGUE CRACK INITIATION

In Section 2, two methods for the fatigue strengthening of metallic beams were suggested. In the first method, the NM CFRP is pre-stressed, and a compressive force is applied to the metallic member to reduce its fatigue vulnerability. In the second method, the stiffness of the metallic beam is increased such that the stresses are reduced below the fatigue limit. The main question about the first strengthening method is how much pre-stress should be applied to the CFRP laminate to achieve infinite fatigue life. For the second strengthening scheme, the main question is how stiff the CFRP laminates should be to reduce the stress to below the fatigue limit. To quantify the magnitude of the required CFRP pre-stress and Young's modulus in each of these methods, the behavior of the beams strengthened by the bonded pre-stressed CFRP laminates will be modeled in this section.

Consider a steel beam with a symmetrical cross-section that is strengthened by a pre-stressed CFRP laminate in the four-point bending set-up shown in Fig. 3. The span length of the beam is L, and the length of the CFRP plate is L_p. The distance between the support to the end of the laminate is a, and the distance between the support to the concentrated load is b. Note that in Fig. 3, the coordinate system is placed at the right end of the CFRP laminate; therefore, 'x' indicates the longitudinal distance from the laminate end. Figure 4 shows a differential segment dx of the laminated metallic beam. Note that the subscripts 's' and 'p' denote terms related to the steel and the CFRP plate, respectively, and the superscripts M and N are associated with the terms related to the bending and longitudinal forces at the neutral plane for each adherend, respectively. The governing differential equations of the laminated beam can be developed as described in Ghafoori (2015). Finally, the stress at the outermost fiber in the lower flange as function of x can be written as (Ghafoori 2015)

$$\sigma(x) = M_T(x)\frac{h}{2I_s} - \frac{b_p}{\lambda^2}\left(\frac{h^2}{4I_s} + \frac{1}{A_s}\right)\left(\frac{d\tau(x)}{dx} + m_1\lambda^2 M(x) + \frac{G_a N_0}{t_a E_p A_p}\right) \quad (2)$$

where

$$\lambda = \sqrt{\frac{G_a b_p}{t_a}\left(\frac{1}{E_s A_s} + \frac{1}{E_p A_p} + \frac{h^2}{4E_s I_s}\right)} \quad (3)$$

and

$$m_1 = \frac{G_a}{2t_a\lambda^2}\frac{h}{E_s I_s} \quad (4)$$

where G_a is the shear modulus of the adhesive layer and N_0 is the initial pre-stressing force in the laminate.

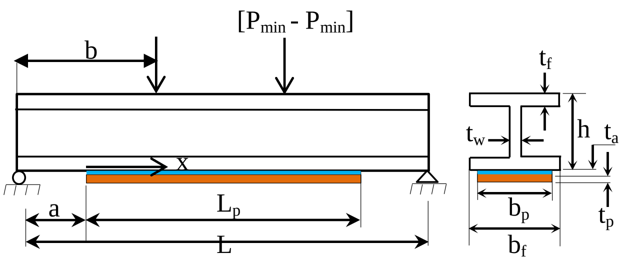

Fig. 3. Beam strengthened by the bonded CFRP laminate in a four-point bending set-up.

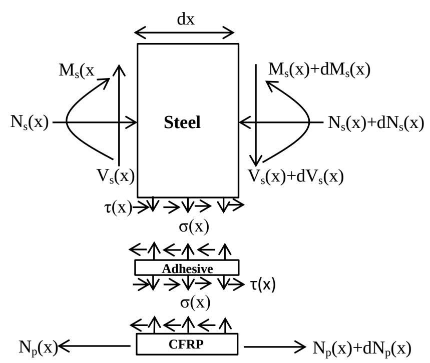

Fig. 4. Equilibrium in an infinitesimal element (Ghafoori 2015).

The method presented in the last section gives the stress at the beam bottom flange. The maximum bending moment, which is located at the beam mid-span (i.e., $x=L_p/2$), is $M_t(L_p/2)=Pa$; thus, based on Eq. (2), the stress at the beam bottom flange can be expressed by

$$\sigma(L_p/2) = \frac{hPa}{2I_s} - b_p\left(\frac{h^2}{4I_s} + \frac{1}{A_s}\right)\left(-\frac{\tau(L_p/2)}{\lambda} + m_1 Pa + \frac{G_a N_0}{\lambda^2 t_a E_p A_p}\right) = \sigma \quad (5)$$

where $\tau(L_p/2)$ is the interfacial shear stress at the beam's mid-span, which is zero in this case. For more details about development of Eq. (5), the reader is referred to Ghafoori (2015). Assume that the strengthened beam is subjected to cyclic loading with minimum and maximum external load levels of P_{min} and P_{max}, respectively, as shown in Fig. 3. The maximum and the minimum stresses at the beam mid-span can be determined using Eq. (5). The mean and amplitude stresses at the beam bottom flange are expressed by

$$\sigma_{\mathrm{m}} = \frac{haP_{\mathrm{m}}}{2I_s} - b_p\left(\frac{h^2}{4I_s} + \frac{1}{A_s}\right)\left(m_1 aP_{\mathrm{m}} + \frac{G_a N_0}{\lambda^2 t_a E_p A_p} e^{-\lambda L_p/2}\right) \tag{6}$$

and

$$\sigma_a = \frac{haP_a}{2I_s} - b_p\left(\frac{h^2}{4I_s} + \frac{1}{A_s}\right)\left(m_1 aP_a + \frac{G_a N_0}{\lambda^2 t_a E_p A_p}\right) \tag{7}$$

where P_a and P_m are, respectively,

$$P_a = \frac{P_{\max} - P_{\min}}{2} \tag{8.a}$$

and

$$P_m = \frac{P_{\max} + P_{\min}}{2} \tag{8.b}$$

The magnitude of the stress at the edge of the hole is written by

$$\sigma^h = k_{tot}\sigma, \tag{9}$$

where k_{tot} is given by

$$k_{tot} = k_f \frac{b_f}{b_f - d} \tag{10}$$

In Eq. (10), d is the diameter of the hole and k_f is the fatigue stress concentration factor (SCF), which depends on the geometry and the material of the member and can be found by formulation given in Ghafoori et al. (2015a). For simplicity in design purposes, a conservative factor of k_f=3 can be approximated for fatigue SCF. Substitution of Eqs. (6) and (7) into Eq. (10) yields the mean, σ_m^h, and the amplitude, σ_a^h, stresses at the location of the hole. The obtained mean and amplitude stresses are the critical stresses and are substituted into the Goodman criterion in Eq. (1), which results in

$$\begin{aligned} &\frac{haP_a}{2I_s S_e} - \frac{b_p}{S_e}\left(\frac{h^2}{4I_s} + \frac{1}{A_s}\right)\left(m_1 aP_a + \frac{G_a N_0}{\lambda^2 t_a E_p A_p}\right) + \frac{haP_{\mathrm{m}}}{2I_s S_{ut}} \\ &-\frac{b_p}{S_{ut}}\left(\frac{h^2}{4I_s} + \frac{1}{A_s}\right)\left(+m_1 aP_{\mathrm{m}} + \frac{G_a N_0}{\lambda^2 t_a E_p A_p} e^{-\lambda L_p/2}\right) \le \frac{b_p - d}{n b_p k_f} \end{aligned} \tag{11}$$

Equation (11) can be solved in terms of different parameters such as pre-stress, N_0, CFRP Young's modulus, E_p, laminate thickness, t_p, and laminate width, b_p. The solution gives the magnitude of the parameter to be used in the strengthening design, such that the stresses are shifted inside the fatigue safe region based on the Goodman criterion. Note that the equality form of Eq. (11) gives the minimum magnitude of the design parameter, whereas the inequality form of Eq. (11) gives a range for the magnitude of the design parameter that can shift the stresses inside the safe zone (i.e., blue region in Fig. 1).

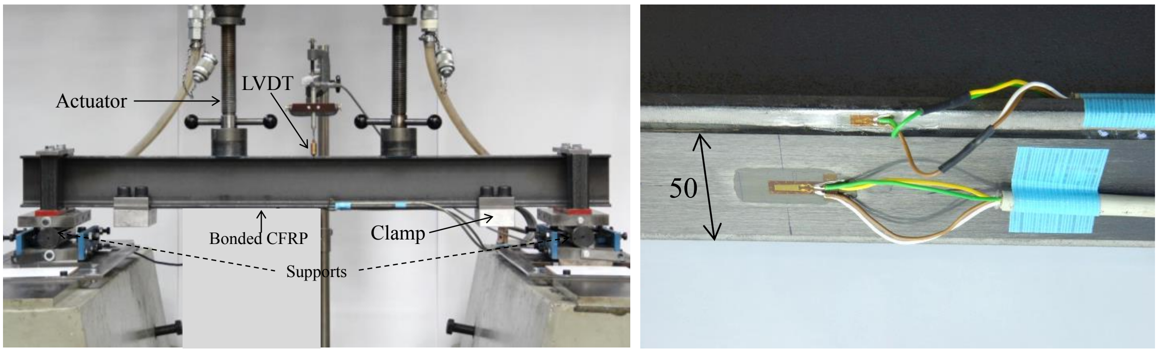

(a) (b)

Fig. 5. (a) Fatigue test set-up, (b) strain gauges were glued on the laminate and the bottom flange of specimen B1.

4 EXPERIMENTS

4.1 Fatigue test set-up and specimens

Four specimens were prepared and strengthened with non-prestressed CFRP laminates with different Young's moduli, as shown in Table 3. All beams were tested in a four-point bending set-up with a loading span of L=1,200 mm, a shear span of b=400 mm and a CFRP laminate length of L_p=920 mm (i.e., a=140 mm). The material and the geometric properties of the steel beams, the CFRP laminate and the adhesive layer are described as follows: b_f=65 mm, t_f=6.2 mm, t_w=4.4 mm, h=120 mm, t_p=1.4 mm, b_p=50 mm, t_a=1 mm, E_s=199.3 GPa and G_a=1,040 MPa. The Young's modulus of the NM, HM and UHM laminates are E_p^{NM} =159 GPa, E_p^{HM} =220 GPa and E_p^{UHM} =440 GPa.

All beams were tested using the symmetric four-point bending set-up shown in Fig. 5.a. Figure 5.a also shows the state of the supports and hydraulic actuators. For all of the fatigue tests, a loading frequency of 4.35 Hz was maintained. Two small holes, each with a diameter of 3 mm, were drilled on bottom flange at mid-span to create stress concentrations to initiate fatigue cracks while also simulating the effect of rivet holes in riveted bridges. Special attention was paid during the drilling of the holes, and quality control was ensured using non-destructive testing (NDT) methods to verify the surface condition of the holes between specimens. For all fatigue strengthened specimens, three strain gauges were glued on the laminate, one at the symmetry line, and two at distances of 200 mm and 300 mm from the symmetry line. One additional strain gauge was applied on the beam's bottom flange, as shown in Fig. 5.b. By using the method presented in Ghafoori et al. (2015a), the fatigue SCF for each hole at the beam bottom flange is found to be k_f=2.35. From Eq. (10), the total SCF is calculated to be k_{tot}=2.59.

The endurance limit was also determined by using Marin's method described in Ghafoori et al. (2015a) to be S_e =220 MPa. All specimens were subjected to an elastic cyclic loading range of P=[1.7-18] kN.

5 RESULTS

First, the unstrengthened reference specimen, B0, was subjected to a cyclic loading. The fatigue loading was stopped in intervals of approximately 10k cycles for an NDT inspection. The Eddy Current NDT system was used to inspect the area near the hole region to detect the formation of any cracks. The Eddy Current system works based on the electromagnetic induction of circular coils and is often used to find flaws down 0.5 mm in conductive metals.

A fatigue crack was initiated from the hole at the beam bottom flange after 448,000 cycles. Note that the main goal of this study is to prevent fatigue crack initiation; thus, as soon as a crack was detected, the specimen was considered to have failed.

Table 1. Fatigue test results.

Specimen	Retrofit scheme	Laminate type	Cycles to failure	Failure mode
B0	Unstrengthened	-	448,000	Crack initiation
B1	Bonded	NM CFRP	1,705,000	Crack initiation
B2	Bonded	HM CFRP	2,000,000	Runout
B3	Bonded	UHM CFRP	2,000,000	Runout

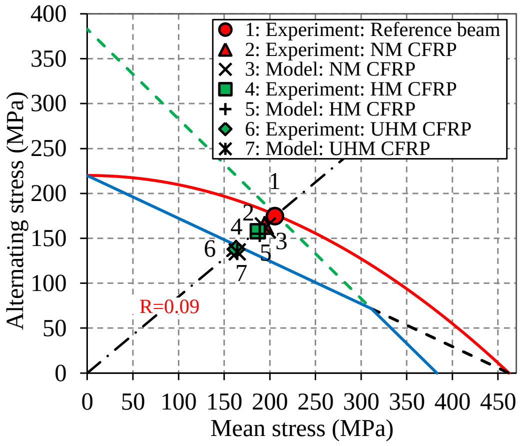

Fig. 6. Comparison between the experimental and modeling results. As the CFRP Young's modulus increases, the stresses approach the safe zone along the stress ratio line R=0.09 .

Specimen B1 was strengthened using the NM CFRP laminate and was then subjected to cyclic loading. The fatigue crack initiated from the hole after 1,705,000 cycles. Similar to the reference specimen, the crack first propagated in the bottom flange and later into the web. Due to the high interfacial shear stresses at the adhesive layer near the damaged section (i.e., at $x=L_p/2$), CFRP-to-steel debonding occurred at the middle of the CFRP laminate and propagated towards the laminate ends. After the CFRP laminate was debonded, the overall SIF at the crack tip exceeded the mode-I fracture toughness of steel and a sudden failure occurred.

The different failure stages are schematically shown in Fig. 7. Stage 1 depicts the crack initiation phase, in which microcracks are nucleated. Because of the influence of microstructures (e.g., grain boundaries) in stage 1, the propagation of microcracks can be erratic and very slow. Nonetheless, after some further microcrack growth away from the nucleation site, a more regular crack growth will occur, which is the commencement of the macrocrack FCG (see stage 2). Note that although crack growth occurs in both stages 1 and 2, differentiating between these two stages is very important because the parameters that are affecting each stage are different. For example, surface conditions have a significant influence on the initiation phase (stage 1); however, they have negligible effects on the crack growth phase (stage 2). Note that the crack initiation phase (stage 1) is assumed to be completed when the crack growth is no longer dependent on the surface conditions. From a theoretical point of view, stage 1 is associated with the fatigue resistance design approach based on the concept of the fatigue limit (i.e., the classical fatigue analysis using S-N curve approach) whereas stage 2 is related to the fatigue crack problem within the context of fracture mechanics. For the structural metals, the duration of the crack initiation stage is much larger than the FCG (often reaching 80% of the total life). Stage 3 in Fig. 7 indicates the CFRP-to-steel debonding, which occurred due to the high interfacial shear stress at the adhesive joint under the damaged section. Eventually, a sudden "brittle" failure of the structural element occurs in the steel section (stage 4). Note that the main aim of the method presented in this paper is to develop a method to increase the duration of the crack initiation stage (i.e., stage 1) to infinity by reducing the applied stresses below the material fatigue limit.

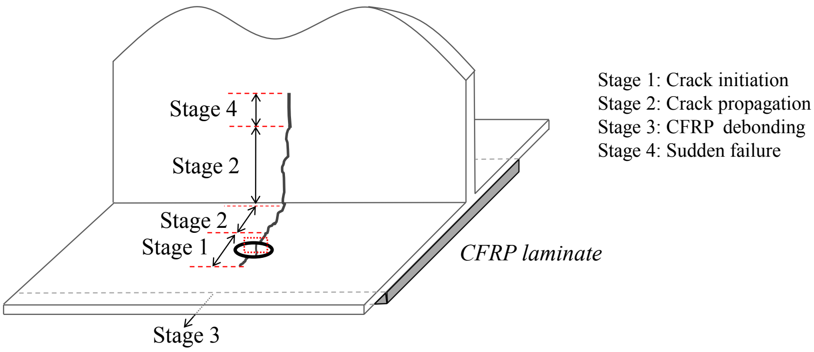

Fig. 7. Schematic view of the crack initiation phase (stage 1), the crack propagation phase (stage 2), the CFRP-to-steel debonding (stage 3) and the sudden fracture (stage 4) (Ghafoori 2015).

Specimen B2 was strengthened using the HM laminate and was then subjected to cyclic loading. The specimen survived more than 2,000,000 cycles and no crack was detected (using the Eddy current system) near the holes in the bottom flange. Furthermore, specimen B3 was strengthened using the UHM laminate and was subjected to cyclic loading. The specimen survived more than 2,000,000 cycles and no crack was found at the location of the holes.

Table 1 shows the number of cycles applied to each specimen and the corresponding failure mode. Figure 6 shows the stresses in the reference specimen and in the specimens strengthened by the NM, the HM and the UHM CFRP laminates in the CLD. The results from the experiments are compared with those obtained from the presented analytical model. It is seen that as the stiffness of the laminate increases, the stresses approach the safe region along the stress ratio line R=0.09, which verifies the assumption made in the presented model. In Fig. 6, the red markers represent the failed specimens, whereas the green markers indicate the survivors after 2,000,000 cycles.

6 CONCLUSIONS

The principle of the CLD approach was described. The influence of different parameters, such as the pre-stress level, geometric and mechanical properties of the CFRP laminate on both the static and fatigue behavior of the retrofitted beam, was discussed. Different mechanisms by which the CFRP laminates can shift the stresses from the risky finite-life region to the safe infinite-life region were explained. A total of four steel beams were tested, including one unstrengthened beam and four strengthened beams. The following conclusions were determined from the analytical and experimental studies:

1) The two main mechanisms that shift the detail from the risky finite-life regime to the safe infinite-life regime were identified:
   a) Mechanism 1: by applying a pre-stress force to an existing fatigue-susceptible detail, the mean stress level and the stress ratio, R, will be reduced such that the detail is shifted from the finite-life regime to the infinite-life regime.
   b) Mechanism 2: by increasing the stiffness of the beam (e.g., by using the UHM CFRP laminates), the stress ratio, R, is preserved, but the mean and alternating stresses will be reduced such that the detail is shifted from the finite-life regime to the infinite-life regime.
2) The method can determine the required CFRP pre-stress and/or the CFRP Young's modulus based on the stress history from the current traffic loadings on the bridge, to prevent future fatigue crack initiation.
3) The qualitative results of the analytical method were compared with the laboratory results of a series of fatigue experiments. The minimum required CFRP Young's modulus determined from the CLD analysis corresponded with observed experimental results.
4) The proposed method can be used particularly for the fatigue strengthening of metallic structures with unknown stress history from past traffic loadings.

7 REFERENCE

Budynas, R. G. & Nisbett, J. K. 2008. *Shigley's Mechanical Engineering Design,* New York, McGraw-Hill.

Colombi, P., Bassetti, A. & Nussbaumer, A. 2003. Analysis of cracked steel members reinforced by pre-stress composite patch. *Fatigue and Fracture of Engineering Materials and Structures,* 26**,** 59-66.

Ghafoori, E. 2015. *Fatigue strengthening of metallic members using un-bonded and bonded CFRP laminates.* PhD Thesis, ETH Diss. No. 22645, ETH Zurich, Switzerland.

Ghafoori, E., Motavalli, M., Nussbaumer, A., Herwig, A., Prinz, G. & Fontana, M. 2015a. Determination of minimum CFRP pre-stress levels for fatigue crack prevention in retrofitted metallic beams. *Engineering Structures,* 84**,** 29–41.

Ghafoori, E., Motavalli, M., Nussbaumer, A., Herwig, A., Prinz, G. S. & Fontana, M. 2015b. Design criterion for fatigue strengthening of riveted beams in a 120-year-old railway metallic bridge using pre-stressed CFRP plates. *Composites Part B,* 68**,** 1-13.

Täljsten, B., Hansen, C. S. & Schmidt, J. W. 2009. Strengthening of old metallic structures in fatigue with prestressed and non-prestressed CFRP laminates. *Construction and Building Materials*, 23**,** 1665-1677.

Wu, C., Zhao, X. L., Al-Mahaidi, R., Emdad, M. R. & Duan, W. H. 2013. Fatigue tests on steel plates with longitudinal weld attachment strengthened by ultra high modulus carbon fibre reinforced polymer plate. *Fatigue and Fracture of Engineering Materials and Structures,* 36**,** 1027-1038.